Spiral Defect Chaos in a Model of Rayleigh-Bénard Convection

Hao-wen Xi and J. D. Gunton
Department of Physics, Lehigh University, Bethlehem, Pennsylvania 18015

Jorge Viñals
Supercomputer Computations Research Institute, B-186, Florida State University, Tallahassee, Florida 32306-4052
and Department of Chemical Engineering, B-203,
Florida Agricultural and Mechanical University/Florida State University College of Engineering,
Tallahassee, Florida 32316-2185
(Received 17 May 1993)

A numerical solution of a generalized Swift-Hohenberg equation in two dimensions reveals the existence of a spatiotemporal chaotic state comprised of a large number of rotating spirals. This state is observed for a reduced Rayleigh number $\epsilon = 0.25$. The power spectrum of the pattern is isotropic, and the spatial correlation function decays exponentially, with an estimated decay length $\xi \approx 2.5\lambda_c$, where λ_c is the critical wavelength near the onset of convection. Our study suggests that this spiral defect state occurs for low Prandtl numbers and large aspect ratios.

PACS numbers: 47.20.Bp, 47.27.Te

The spatiotemporal chaotic behavior of spatially extended, dissipative systems has been intensively studied in recent years [1]. The transition to spatiotemporal chaos has been observed in various physical systems such as Rayleigh-Bénard convection [2], optical instabilities [3], flames [4], and chemical reactions [5]. Spatiotemporal chaos manifests itself through a breakdown of global spatial coherence. However, a macroscopic *coherence length*—a length scale below which the pattern appears coherent—may still be observed. This form of chaos is often referred to as *weak turbulence*. Recently, a chaotic spiral defect pattern (which we will refer to loosely as spiral chaos below) has been observed in Rayleigh-Bénard convection in a non-Boussinesq fluid (CO_2 gas) [6], for a large aspect ratio and at moderate Rayleigh numbers. In previous experiments on convection in CO_2 gas [7], the spontaneous formation of a stable rotating spiral pattern was observed at a lower Rayleigh number. The chaotic state observed more recently [6] is comprised of a large number of rotating spirals. Spirals nucleate, interact, and annihilate yielding a macroscopically disordered pattern. In this paper, we show that a generalized Swift-Hohenberg equation which includes a quadratic nonlinearity and coupling to mean flow can account for the formation of this chaotic spiral pattern. We find that chaotic spiral patterns are spontaneously formed during the transition from the conduction state to rolls, in agreement with the experimental observations.

In order to distinguish among temporal chaos (for systems with a few spatial degrees of freedom), spatiotemporal chaos (for systems with many spatial degrees of freedom) and fully developed turbulence, we summarize a scenario proposed by Hohenberg and Shraiman [8]. Consider the following length scales for a system: the linear system size L, the correlation length ξ, the excitation length l_E (the characteristic length at which energy is introduced into the system), and the dissipation length l_D [9] (the characteristic length below which the modes are damped). For example, near the onset of Rayleigh-Bénard convection in an infinite system, $l_D \approx k_c^{-1}$, where k_c is the critical wave number. The excitation length $l_E \approx d \approx k_c^{-1}$, where d is the thickness of the fluid layer. Temporal chaos then corresponds to the case of a small aspect ratio and moderate values of the reduced Rayleigh number R/R_c (where R_c is the critical Rayleigh number), where $L \approx l_D \approx l_E$, so that only a few degrees of freedom are relevant. Fully developed turbulence, on the other hand, occurs for $R/R_c \gg 1$, for which $l_D \ll l_E$. Spatiotemporal chaos occurs at moderate R/R_c, for a large aspect ratio system, with $L \gg l_E \approx l_D \approx d$, and $L \gg \xi$. In this case the system may exhibit spatiotemporal chaos, where one has to deal with many spatial degrees of freedom with local order on a length scale ξ.

We model convection in a non-Boussinesq fluid by a two-dimensional generalized Swift-Hohenberg model [10,11], defined by Eqs. (1)–(4) below, which we solve by numerical integration. The Swift-Hohenberg equation and various generalizations of it have proven to be quite successful in explaining many of the features of convective flow in fluids, particularly near onset [12–16]. As we show in this paper, the same holds true for the formation of spiral chaos in non-Boussinesq fluids. Our model is defined in dimensionless units by

$$\frac{\partial\psi(\mathbf{r},t)}{\partial t} + g_m\mathbf{U}\cdot\boldsymbol{\nabla}\psi = [\epsilon' - (\nabla^2+1)^2]\psi - g_2\psi^2 - \psi^3, \tag{1}$$

$$\left[\frac{\partial}{\partial t} - \mathrm{Pr}(\nabla^2 - c^2)\right]\nabla^2\zeta = [\boldsymbol{\nabla}(\nabla^2\psi)\times\boldsymbol{\nabla}\psi]\cdot\hat{\mathbf{e}}_z, \tag{2}$$

where $\mathbf{U}$ is the mean flow velocity,

0031-9007/93/71(13)/2030(4)$06.00

$$\mathbf{U} = (\partial_y \zeta)\hat{\mathbf{e}}_x - (\partial_x \zeta)\hat{\mathbf{e}}_y. \quad (3)$$

The boundary conditions are

$$\psi|_B = \hat{\mathbf{n}} \cdot \nabla\psi|_B = \zeta|_B = \hat{\mathbf{n}} \cdot \nabla\zeta|_B = 0, \quad (4)$$

where $\hat{\mathbf{n}}$ is the unit normal to the boundary of the domain of integration, B. Equation (1) with $g_2 = g_m = 0$ reduces to the Swift-Hohenberg (SH) equation. The scalar order parameter $\psi(\mathbf{r}, t)$ is related to the fluid temperature in the midplane of the convective cell and $\zeta(\mathbf{r}, t)$ is the vertical vorticity potential. Mean flow arises when the vertical vorticity is driven by roll curvature and amplitude modulations. Coupling to mean flow has been shown to play a key role, for example, in the onset of weak turbulence in Boussinesq fluids [11,17,18]. The quantity ϵ' is the scaled control parameter, $\epsilon' = (\frac{4}{k_c^2 \xi_0^2})\epsilon$, where $\epsilon = \frac{R}{R_c} - 1$ is the reduced Rayleigh number. Here R is the Rayleigh number, R_c is the critical Rayleigh number for an infinite system, k_c is the critical wave number, ξ_0 is the characteristic length scale, Pr is the Prandtl number, and c^2 is an unknown constant.

The values of the parameters that enter the equation have been chosen in the range appropriate for the earlier experiments of Bodenschatz *et al.* on CO_2 [7]. In order to estimate them in terms of experimentally measurable quantities, we have derived a three mode amplitude equation from the generalized Swift-Hohenberg equation [15]. From the experiments described in [7], we have estimated $g_2 \approx 0.35$ and $g_m \approx 50$. The value of ϵ' used in the numerical simulation is 0.7, which is related to the experimental value ϵ in Ref. [7] by $\epsilon = 0.3594\epsilon' = 0.2516$. We have chosen $c^2 = 2$ to simulate approximately the experimental rigid-rigid boundary condition. (Note that $c^2 = 0$ corresponds to a free-free boundary condition.) We note that for these values of the parameters, the classical work of Busse [19] on the stability of various convective states in an infinite fluid predicts that the stable pattern is a set of parallel rolls.

In the numerical calculations we consider a circular cell of radius $R = 32\pi$, which corresponds to an aspect ratio $\Gamma = R/\pi = 32$. A square grid with N^2 nodes has been used with spacing $\Delta x = \Delta y = 64\pi/N$, and $N = 512$. We approximate the boundary conditions on ψ by taking $\psi(\mathbf{r}, t) = 0$ for $\|\mathbf{r}\| \geq R$, where $\mathbf{r}$ is the location of a node with respect to the center of the domain of integration. In order to study the formation of the chaotic spiral pattern from the conducting state, we choose as initial condition $\psi(\mathbf{r}, t = 0)$ a random variable, Gaussianly distributed with zero mean and a variance 0.001.

Our main result is that this model exhibits a spatiotemporal chaotic spiral pattern which is remarkably similar to that observed experimentally [6] (there the system was quenched from the conduction state as well). Figure 1 shows a typical configuration that we have obtained exhibiting spiral chaos. Dark regions correspond to hot rising fluid and white regions to cold descending fluid. Initially, after the control parameter is quenched into the regime in which spiral chaos arises, the randomness in the initial configuration is rapidly lost. On a time scale $t \approx 600$, the system self-organizes into a regular structure comprising locally rotating spirals that fill the entire cell.

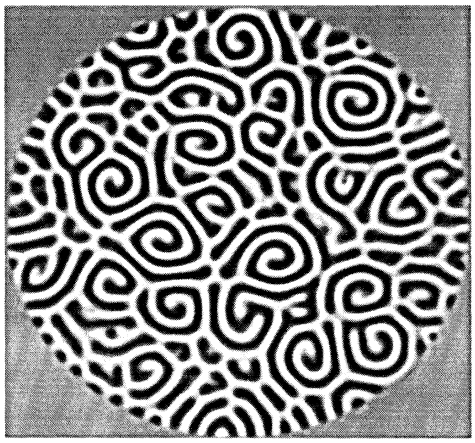

FIG. 1. Typical configuration of a spiral chaos pattern. The field ψ is shown. Dark regions correspond to $\psi > 0$ and light regions to $\psi < 0$. The configuration shown has evolved from random initial conditions in a cylindrical cell with aspect ratio $\Gamma = 32$. The values of the parameters used are $g_2 = 0.35$, $g_m = 50$, and $c^2 = 2$. The parameter ϵ is quenched from 0 to 0.7 in the simulation. The configuration shown is at $t = 900 \approx t_h$.

The two dimensional power spectrum $\langle P(\mathbf{k}) \rangle$ of $\psi(\mathbf{r}, t)$ for spiral chaos is shown in Fig. 2(a), where $\langle\ \rangle$ denotes a time average over one horizontal-diffusion time [20]. The most interesting feature is that the intensity of the spectrum appears to be isotropic. Figure 2(b) shows the circularly averaged power spectrum $P(k)$. We see that $P(k)$ is broad, skewed, and peaked at a wave number $k_{\max} < k_c = 1$. In order to estimate the width of $P(\mathbf{k})$ we have fitted it to a function of the form $A/[1+\xi^4(k^2-k_0^2)^2]$. The fit obtained is shown in Fig. 2(b) as well, and corresponds to $A \approx 7.0$, $\xi \approx 2.4$, and $k_0 \approx 0.8$. The function $P(\mathbf{k})$ is more sensitive to position correlations than orientation correlations in the pattern. The dependence of a correlation function that would measure orientation correlations on the distance need not be the same as that of $C(\mathbf{r})$ [21], which is the inverse transform of $\langle P(\mathbf{k}) \rangle$.

We finally show in Fig. 3 the field ζ that corresponds to the configuration shown in Fig. 1. White and dark regions correspond to clockwise and counterclockwise rotations, respectively. The Fourier transform of this field shows, as expected, that it is peaked around $k = 0$ and is isotropic.

Our numerical investigation indicates that both large scale mean flow and large aspect ratio play a crucial role in the spontaneous formation of a spiral chaos state. In the absence of the mean flow field, we do not observe it.

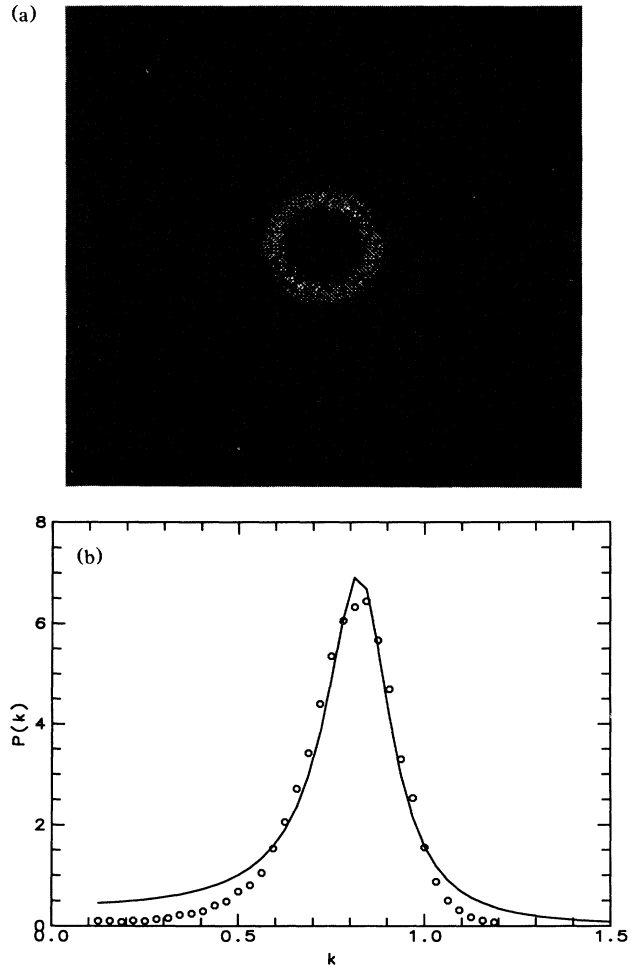

FIG. 2. (a) Power spectrum in **k** space. The intensity of the spectra is approximately isotropic. (b) Circularly averaged power spectrum. The wave number k is in units of k_c, where $k_c = 1$ is the critical wave number. The solid line is the fit discussed in the text.

To study how the spiral chaos state depends on the size of the system, a run was conducted in a small cell of aspect ratio 16. We observed a globally ordered pattern consisting of one two-armed spiral, which demonstrates that a large aspect ratio is critical to the existence of spiral chaos. We have also studied the role of non-Boussinesq effects on the formation of the spiral chaos state. If the non-Boussinesq coupling constant $g_2 = 0$, and we start with the same random initial condition and use the same parameters ($\epsilon' = 0.7$, $g_m = 50, \mathrm{Pr} = 1.0$, and $c^2 = 2.0$), we observe a similar spiral chaos state, demonstrating that the term that models non-Boussinesq effects is not necessary for spiral chaos. We have also carried out additional calculations to study the effect of the Prandtl number. Starting with exactly the same initial conditions and parameters as in Fig. 1, but with a larger value of

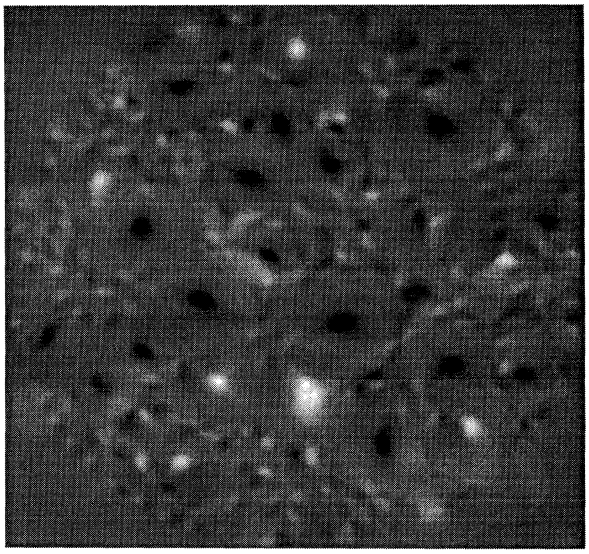

FIG. 3. Vorticity potential field ζ corresponding to the configuration shown in Fig. 1. White and dark regions correspond to clockwise and counterclockwise rotations, respectively.

the Prandtl number ($\mathrm{Pr} = 6$), no spiral chaos pattern is observed, showing that a low Prandtl number is essential for spiral chaos. The resulting pattern has a labyrinthine aspect. Finally, in order to study how generic the spiral chaos states is, we have studied the case in which the system was ramped slowly from a conduction state to a convection state. We used exactly the same initial conditions and the same parameters in Fig. 1, but increased ϵ very slowly up to $\epsilon = 0.7$: $\epsilon = 10^{-3}t$ for $0 < t < 700$ and $\epsilon = 0.7$ for $t > 700$. A similar spiral chaos is observed to form as time increases, although rolls tend to persist near the cell boundary. These results suggest that only the low Prandtl number and large aspect ratio are relevant for the existence of spiral chaos.

We wish to thank E. Bodenschatz, G. Ahlers, and D. Cannell for suggesting the numerical investigation of the generalized Swift-Hohenberg equation and also thank them, and S. Morris, H. S. Greenside, and P. C. Hohenberg, for many stimulating conversations and comments. This work was supported in part by the National Science Foundation under Grant No. DMR-9100245. This work is also supported in part by the Supercomputer Computations Research Institute, which is partially funded by the U.S. Department of Energy Contract No. DE-FC05-85ER25000. The calculations reported here have been carried out on the Cray Y-MP at the Pittsburgh Supercomputing Center.

[1] M.C. Cross and P.C. Hohenberg, Rev. Mod. Phys. **65**, 3 (1993).

[2] G. Ahlers and R.P. Behringer, Prog. Theor. Phys. Suppl. **64**, 186 (1978); G. Ahlers, D.S. Cannell, and V. Steinberg, Phys. Rev. Lett. **54**, 1373 (1985); M.S. Heutmaker and J.P. Gollub, Phys. Rev. A **35**, 242 (1987); P. Manneville, *Dissipative Structures and Weak Turbulence* (Academic, New York, 1990).

[3] F.T. Arecchi, G. Giacomelli, P.L. Rammazza, and S. Risidori, Phys. Rev. Lett. **65**, 1579 (1990); J.V. Moloney and A. Newell, Physica (Amsterdam) **44D**, 1 (1990).

[4] P. Clavin, in *Physico Chemical Hydrodynamics*, edited by M. Velarde (Plenum, New York, 1988).

[5] G. Nicolis and I. Prigogine, *Self-Organization in Nonequilibrium Systems* (Wiley, New York, 1977); H.L. Swinney and V.I. Krinsky, Physica (Amsterdam) **49D**, 1 (1991); G.S. Skinner and H. Swinney, Physica (Amsterdam) **48D**, 1 (1991).

[6] S. Morris, E. Bodenschatz, D.S. Cannell, and G. Ahlers, preceding Letter, Phys. Rev. Lett. **71**, 2026 (1993).

[7] E. Bodenschatz, J.R. de Bruyn, G. Ahlers, and D.S. Cannell, Phys. Rev. Lett. **67**, 3078 (1991).

[8] P.C. Hohenberg and B.I. Shraiman, Physica (Amsterdam) **37D**, 109 (1989).

[9] In general one expects l_D to decrease as R/R_c increases.

[10] J. Swift and P.C. Hohenberg, Phys. Rev. A **15**, 319 (1977).

[11] P. Manneville, J. Phys. (Paris) **44**, 759 (1983).

[12] H.S. Greenside, W.M. Coughran, Jr., and N. L. Schryer, Phys. Rev. Lett. **49**, 726 (1982); H.S. Greenside and W.M. Coughran, Jr., Phys. Rev. A **30**, 398 (1984); H.S. Greenside and M.C. Cross, Phys. Rev. A **31**, 2492 (1985).

[13] M.C. Cross, Phys. Fluids **23**, 1727 (1980); Phys. Rev. A **25**, 1065 (1982); **27**, 490 (1983).

[14] Hao-Wen Xi, J. Viñals, and J.D. Gunton, Physica (Amsterdam) **177A**, 356 (1991); J. Viñals, Hao-Wen Xi, and J.D. Gunton, Phys. Rev. A **46**, 918 (1992).

[15] Hao-Wen Xi, J. Viñals, and J.D. Gunton, Phys. Rev. A **46**, R4483 (1992); Hao-Wen Xi, J.D. Gunton, and J. Viñals, Phys. Rev. E **47**, R2987 (1993); Hao-Wen Xi, J.D. Gunton, and J. Viñals; "Pattern formation during Rayleigh-Bénard convection in non-Boussinesq fluids" (unpublished).

[16] M. Bestehorn, M. Fantz, R. Friedrich, and H. Haken, Phys. Lett. A **174**, 48 (1993).

[17] E.D. Siggia and A. Zippelius, Phys. Rev. Lett. **47**, 835 (1981); A. Zippelius and E.D. Siggia, Phys. Rev. A **26**, 1788 (1982); Phys. Fluids **26**, 2905 (1983).

[18] H.S. Greenside, M.C. Cross, and W.M. Coughran, Jr., Phys. Rev. Lett. **60**, 2269 (1988).

[19] F.H. Busse, Rep. Prog. Phys. **41**, 1929 (1978).

[20] We note that the horizontal diffusion time is Γ^2.

[21] K.R. Elder, J. Viñals, and M. Grant, Phys. Rev. Lett. **68**, 3024 (1992); Phys. Rev. A **46**, 7618 (1992).

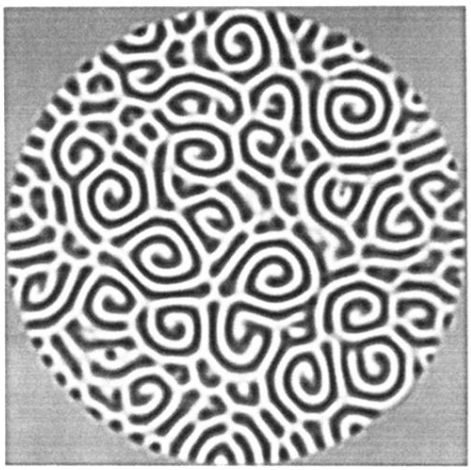

FIG. 1. Typical configuration of a spiral chaos pattern. The field ψ is shown. Dark regions correspond to $\psi > 0$ and light regions to $\psi < 0$. The configuration shown has evolved from random initial conditions in a cylindrical cell with aspect ratio $\Gamma = 32$. The values of the parameters used are $g_2 = 0.35$, $g_m = 50$, and $c^2 = 2$. The parameter ϵ is quenched from 0 to 0.7 in the simulation. The configuration shown is at $t = 900 \approx t_h$.

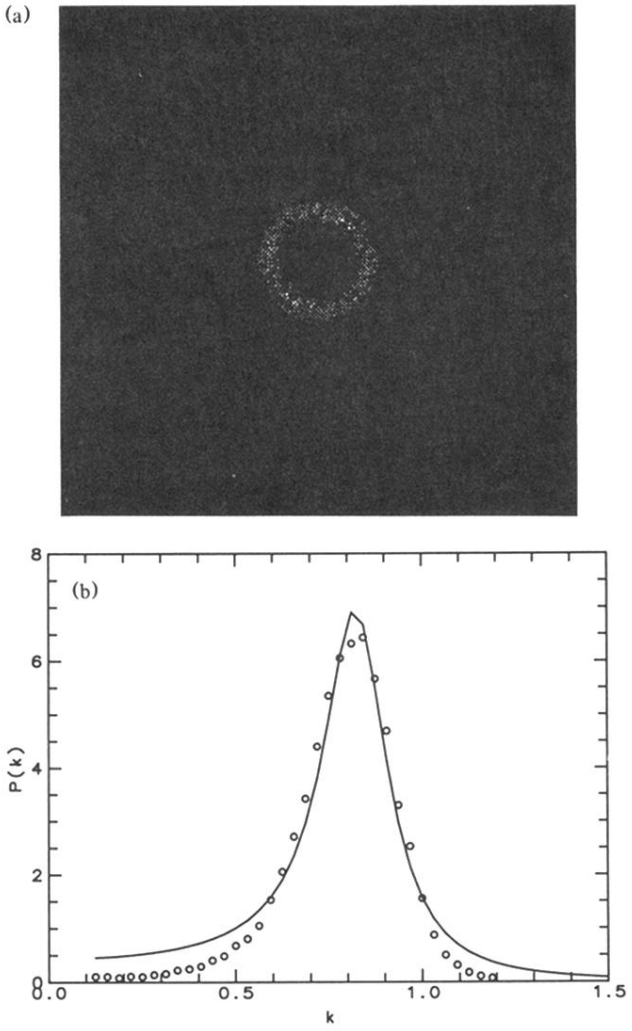

FIG. 2. (a) Power spectrum in **k** space. The intensity of the spectra is approximately isotropic. (b) Circularly averaged power spectrum. The wave number k is in units of k_c, where $k_c = 1$ is the critical wave number. The solid line is the fit discussed in the text.

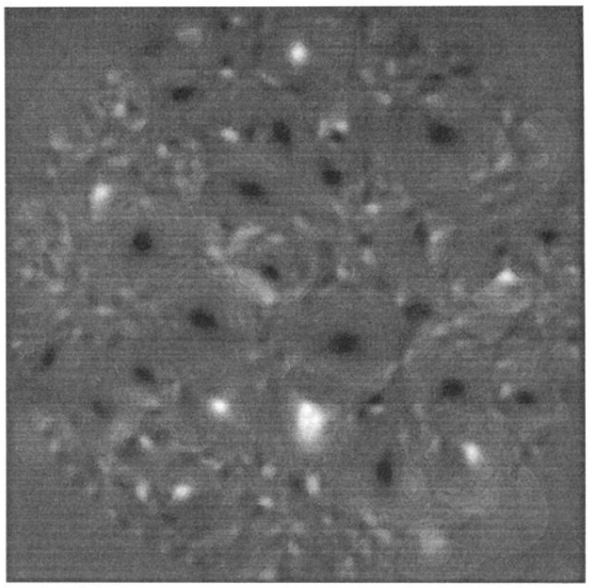

FIG. 3. Vorticity potential field ζ corresponding to the configuration shown in Fig. 1. White and dark regions correspond to clockwise and counterclockwise rotations, respectively.